Universality of the Anderson transition with the quasiperiodic kicked rotor

G. Lemarié[1], B. Grémaud[1,2,3] and D. Delande[1]

[1] *Laboratoire Kastler Brossel, Université Pierre et Marie Curie-Paris 6, ENS, CNRS; 4 Place Jussieu, F-75005 Paris, France*
[2] *IPAL, CNRS; 1 Fusionopolis Way, Singapore 138632, Singapore*
[3] *Centre for Quantum Technologies, National University of Singapore, 3 Science Drive 2, Singapore*

arXiv:0904.2324v1 [cond-mat.dis-nn] 15 Apr 2009

PACS 72.15.Rn – Localization effects (Anderson or weak localization)
PACS 03.75.-b – Matter waves
PACS 71.30.+h – Metal-insulator transitions and other electronic transitions

Abstract. - We report a numerical analysis of the Anderson transition in a quantum-chaotic system, the quasiperiodic kicked rotor with three incommensurate frequencies. It is shown that this dynamical system exhibits the same critical phenomena as the truly random 3D-Anderson model. By taking proper account of systematic corrections to one-parameter scaling, the universality of the critical exponent is demonstrated. Our result $\nu = 1.59 \pm 0.01$ is in perfect agreement with the value found for the Anderson model.

Introduction. – It is now widely acknowledged that the classical diffusive behavior of non-interacting electrons in a disordered potential can be stopped by non-trivial interference effects [1]. This puzzling phenomenon, Anderson localization, constitutes one strong evidence of the very difference between quantum and classical dynamics of complex systems. In the field of quantum chaos, a similar phenomenon is acknowledged, namely dynamical localization. In the kicked rotor, a paradigmatic system of quantum chaos, quantum mechanical interference tend to suppress the classical chaotic diffusive dynamics. The discovery of the parallel between dynamical localization and Anderson localization originated from the mapping of the kicked rotor to the quasirandom 1D Anderson model [2]. In Ref. [3] it was demonstrated that the kicked rotor in the dynamical localization regime could be modeled by random band matrices; the latter have been reduced to a 1D nonlinear σ model [4] similar to those employed in the localization theory [5]. In Ref. [6] the direct correspondence between the kicked rotor and the diffusive supersymmetric nonlinear σ model was demonstrated. In the localized regime, the kicked rotor *exactly* mimics the behavior of disordered electronic conductors.

There has been much efforts to observe Anderson localization in 3D experimentally. However, due to stray effects like interaction, decoherence or absorption, very few attempts have been successful [7]. In a slightly different context, Anderson localization of acoustic [8] and electromagnetic [9–12] waves has been experimentally observed. The experimental realization of the kicked rotor with laser-cooled atoms interacting with a pulsed standing wave allowed for the first experimental observation of Anderson localization in 1D with atomic matter waves [13]. One step further is to observe the well-known Anderson *transition* with this type of system, i.e. the disorder induced metal-insulator transition predicted for non-interacting electrons subjected to a 3D disordered potential. Different generalizations of the kicked rotor have been theoretically considered as analogs of the 3D-Anderson model [14]. Here, we focus on the convenient three-incommensurate-frequencies generalization introduced in Ref. [15]. Very recently an experiment based on this system has fully characterized the Anderson metal-insulator transition [16]. Indeed, a careful analysis of the scaling properties of the dynamics has resulted in the first experimental determination of the localization length critical exponent ν of the Anderson transition. The value found $\nu = 1.4 \pm 0.3$ is compatible with the precedent numerical determination of $\nu = 1.57 \pm 0.02$ for the true-random 3D-Anderson model [17].

At this stage, the equivalence between the quasiperiodic kicked rotor [16] and 3D-disordered conductors still has the status of a conjecture (see [18]). A rigorous answer to the question whether this dynamical system exhibits the same critical phenomena – i.e. belongs to the

same university class – as the true 3D-Anderson model has not yet been given. Can a simple three-frequency dynamical system exactly mimic the critical behavior of 3D disordered electronic conductors? In this Letter, we show that the answer is positive. This is done by carrying out a very precise numerical study of the critical behavior of the quasiperiodic kicked rotor *with the same care* as in the most sophisticated investigations of the critical behavior of the true 3D-Anderson model [17,19,20]. The fact that both models give the same localization length critical exponent ν within comparable (small) uncertainties implies that they belong to the same universality class (orthogonal) [21].

The quasiperiodic kicked rotor. – The quasiperiodic kicked rotor we consider is a three-incommensurate-frequencies generalization of the kicked rotor:

$$H_{qp} = \frac{p^2}{2} + \mathcal{K}(t)\cos\theta \sum_n \delta(t-n) \;, \tag{1}$$

obtained simply by modulating the amplitude of the standing wave pulses with a set of two new incommensurate frequencies ω_2 and ω_3 of modulation:

$$\mathcal{K}(t) = K\left[1 + \varepsilon\cos\left(\omega_2 t + \varphi_2\right)\cos\left(\omega_3 t + \varphi_3\right)\right] \;. \tag{2}$$

Here we consider the case with an effective Planck constant $\hbar = -i[\theta, p]$. For a standard rotor, θ is an angle defined modulo 2π and the wavefunction thus has to be 2π periodic. In the atomic realization of the kicked rotor [16], the Hamiltonian is still given by Eq. (1), with θ extended in the $(-\infty, +\infty)$ range. Using the Bloch theorem, one can restrict to 2π periodic functions, at the (cheap) price of including a constant quasi-momentum.

The dynamics of this quasiperiodic kicked rotor is *identical* to the time-evolution of a 3D-kicked rotor:

$$H_3 = \frac{{p_1}^2}{2} + \omega_2 p_2 + \omega_3 p_3 + K\cos\theta_1\left[1 + \varepsilon\cos\theta_2\cos\theta_3\right]\sum_n \delta(t-n) \;, \tag{3}$$

with an initial condition:

$$\Psi_3(\theta_1,\theta_2,\theta_3,t=0) \equiv \Psi_{qp}(\theta_1,t=0)\delta(\theta_2-\varphi_2)\delta(\theta_3-\varphi_3) \;. \tag{4}$$

where $\Psi_{qp}(\theta, t=0)$ is an arbitrary initial condition for the quasiperiodic kicked rotor. Note that dynamical localization takes place in momentum, not configuration, space. The initial state being perfectly localized in θ_2 and θ_3, it is entirely delocalized in the conjugate momenta p_2 and p_3 so that we will study transport along the p_1 direction, which is tantamount to measure the momentum distribution of the quasiperiodic kicked rotor $|\Psi_{qp}(p,t)|^2$. The unusual linear dependence of H_3 with p_2 and p_3 does not prevent, for nonzero ϵ the dynamics to be similarly diffusive or localized along the 3 coordinates.

The Hamiltonian H_3 is invariant under the transformation $T : t \to -t, \boldsymbol{\theta} \to -\boldsymbol{\theta}, \mathbf{p} \to \mathbf{p}$, i.e. the time-reversal in the momentum representation, which is the relevant one for the dynamical localization (see [22,23]). In particular, the choice of a non-zero quasi-momentum and non-zero phases φ_2 or φ_3 does not break time-reversal symmetry. The evolution of the states according to the Hamiltonian (1) is governed by the operator U [see below Eq. (5)], belonging to the Circular Orthogonal Ensemble class, with the additional constraint at $t = 0$ (4), this shows that the dynamical properties of the present quasiperiodic kicked rotor also belong to the orthogonal ensemble.

It should also be noted that the 3D aspect comes from the fact that 3 frequencies are present in our dynamical system: the usual "momentum frequency" $\hbar$ which is present in the standard kicked rotor (with $\varepsilon = 0$), and the two additional time-frequencies ω_2 and ω_3. By increasing the number of incommensurate frequencies, one should be able to tune the effective dimensionality of the system. This holds the promise of extending the study of the Anderson transition to higher dimensions.

From a stroboscopic point of view, the quantum dynamics of the 3D-kicked rotor Eq. (3) is determined by its evolution operator over one period:

$$U = e^{-iK\cos\theta_1(1+\varepsilon\cos\theta_2\cos\theta_3)/\hbar} \times e^{-i\left(p_1^2/2+\omega_2 p_2+\omega_3 p_3\right)/\hbar} \;, \tag{5}$$

whose eigenstates form a basis set allowing to calculate the temporal evolution. These Floquet states $|\phi\rangle$ are fully characterized by their quasienergy ω, defined modulo 2π:

$$U|\phi_\omega\rangle = e^{-i\omega}|\phi_\omega\rangle \;. \tag{6}$$

Equivalence with a 3D-Anderson tight-binding model can be obtained by reformulating Eq. (6) for the Floquet states [2]:

$$\epsilon_{\mathbf{m}}\Phi_{\mathbf{m}} + \sum_{\mathbf{r}\neq 0} W_{\mathbf{r}}\Phi_{\mathbf{m}-\mathbf{r}} = -W_{\mathbf{0}}\Phi_{\mathbf{m}} \;, \tag{7}$$

where $\mathbf{m} \equiv (m_1, m_2, m_3)$ and $\mathbf{r}$ label sites on a 3D lattice, and the $\Phi_{\mathbf{m}}$ are simply related to the Fourier components of the Floquet state $|\phi_\omega\rangle$. The on-site energy $\epsilon_{\mathbf{m}}$ reads:

$$\epsilon_{\mathbf{m}} = \tan\left\{\frac{1}{2}\left[\omega - \left(\hbar\frac{{m_1}^2}{2} + \omega_2 m_2 + \omega_3 m_3\right)\right]\right\} \;, \tag{8}$$

and the hopping amplitudes $W_{\mathbf{r}}$ are coefficients of a threefold Fourier expansion of $W(\theta) = \tan\left[K\cos\theta_1(1+\varepsilon\cos\theta_2\cos\theta_3)/\,2\hbar\right]$.

When $(\hbar, \omega_2, \omega_3)$ is an incommensurate triplet of frequencies, each component of the triplet being in addition incommensurate with π, the classical dynamics can become chaotic (for sufficiently large stochasticity parameter $K \gtrsim 2$) with diffusive spreading in *all* $\mathbf{m}$ directions [15]. The pseudo-random character of the potential $\epsilon_{\mathbf{m}}$ then gives the disorder in the model (7).

We therefore expect to observe localization effects as predicted for the standard 3D-Anderson model. Localized

states would be observed if the disorder strength is large as compared to the hopping amplitudes. In the case of model (7), while the amplitude of disorder is fixed, the hopping amplitudes increase with K. Therefore, for large K a diffusive regime should be observed, while for small K (though sufficiently large as to prevent classical localization effects) a localized regime is expected. This was validated both numerically [15] and experimentally [16].

Finite-time scaling. – In the case of the kicked rotor, the initial classical chaotic diffusion is stopped only after a certain characteristic time, the localization time τ_ℓ which turns out to be roughly proportional to the localization "length" (characterizing the exponential localization in momentum space) [24]: $\tau_\ell \propto \ell$. In 3D, the localization time scales as $\tau_\ell \sim \ell^3$. Thus for very large localization length, τ_ℓ may exceed the largest time accessible (the maximum duration of a cold-atoms experiment is typically 150 kicks [16] whereas numerical investigations can go up to 10^6 kicks). Consequently, it is vain to investigate the Anderson transition only from static properties of the quasiperiodic kicked rotor, such as the divergence of the localization length at criticality, which could be obtained only for $t \gg \tau_\ell$.

Actually, these finite-time effects are similar to finite-size effects for the study of classical or quantum phase transitions. We can generalize the usual scaling laws to cover our time-dependent problem. The single parameter scaling theory, successfully used for the standard (static) 3D Anderson model [25–27], can be applied to analyze the dynamics (see [16]) and especially to determine the critical properties of the Anderson transition, i.e. the critical exponents.

The dynamics of the quasiperiodic kicked rotor is conveniently studied by considering the time-evolution of the variance of the momentum distribution $\langle p^2 \rangle$. We can make the following scaling hypothesis for this quantity [28]:

$$\langle p^2 \rangle = t^{k_1} F\left[(K - K_c)\, t^{k_2} \right] , \tag{9}$$

with F a function characteristic of the transition which is to be determined and k_1 and k_2 two exponents which can be constrained as explained in the following. K_c is the critical value of the stochasticity parameter. Note that $\langle p^2 \rangle$ is here averaged over several initial conditions (this corresponds to an average over the disorder). We must recover as $t \to \infty$ either a diffusive behavior $\langle p^2 \rangle \sim Dt$ when $K > K_c$ or a localized dynamics $\langle p^2 \rangle \sim \ell^2$ when $K < K_c$. In the vicinity of the transition, the diffusion constant $D \sim (K - K_c)^s$ vanishes with the critical exponent s and the localization length $\ell \sim (K_c - K)^{-\nu}$ diverges with the critical exponent ν. Together with Wegner's law [29] $s = \nu$ in three dimensions, this leads to $k_1 = 2/3$ and $k_2 = 1/3\nu$ [30].

Therefore, to analyze the scaling of the dynamics, the behavior of the quantity $\Lambda = \langle p^2 \rangle t^{-2/3}$ should be investigated as a function of time and for various stochasticity parameters. Such a study was undertaken in [16] and allowed for a successful experimental characterization of the Anderson transition. In order to tackle the problem of universality of the critical behavior, we have to go one step further and study whether the critical exponent ν changes when parameters such as $\bar{k}, \omega_2, \omega_3$ are modified.

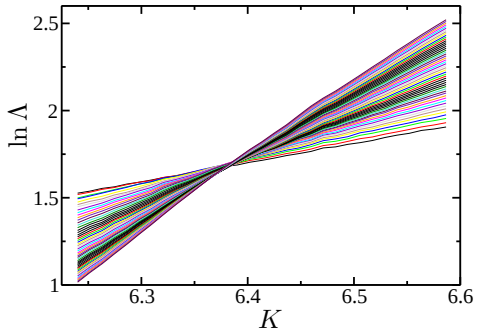

Fig. 1: (Color online) Dynamics of the quasiperiodic kicked rotor in the vicinity of the critical regime. The rescaled quantity $\ln \Lambda(K, t)$ is plotted as a function of K for various values of time t ranging from $t = 30$ to $t = 40000$. The crossing of the different curves at a common point ($K_c \simeq 6.4, \ln \Lambda_c \simeq 1.6$) indicates the occurrence of the metal-insulator transition. The parameters are that of the set $\mathcal{A}$ (see Table 1).

The following discussion is rather intricate but cannot be avoided in a rigorous study. Indeed, to reliably distinguish the different universality classes of the Anderson transition requires a very precise determination of the critical exponent; for instance, the value $\nu = 1.43 \pm 0.04$ for the unitary symmetry class is very close to the one for the orthogonal symmetry class [19]. For a very accurate determination of ν, possible systematic deviations to one-parameter scaling must be taken into account.

Systematic corrections to scaling. – Let us consider the scaling function $\mathcal{F} \equiv \ln F$ in the vicinity of the critical point:

$$\ln \Lambda = \mathcal{F}\left[(K - K_c)\, t^{1/3\nu} \right] . \tag{10}$$

One simple feature of the scaling hypothesis Eq. (10) is that when $\ln \Lambda$ is plotted against K, the curves for different times t should intersect at a common point $(K_c, \ln \Lambda_c)$; this crossing, which indicates the occurrence of the metal-insulator transition, is clearly visible in Fig. 1.

In practice, the data do not exactly follow Eq. (10). There are small systematic deviations to scaling. Here, we consider several ways in which such corrections can arise (see below for a detailed discussion of each correction): (i) the presence of an irrelevant scaling variable, (ii) non-linear dependence of the scaling variables in the stochasticity parameter K and (iii) resonances due to the periods being well approximated by a ratio of small integers. (iii) is specific to our three-frequency dynamical system, but (i) and (ii) were shown to play an important role in the standard Anderson model [17]. Note that the

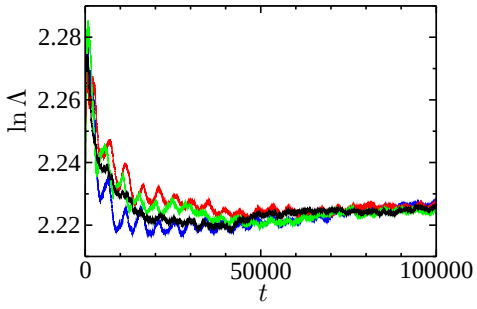

Fig. 2: (Color online) Small oscillating corrections to the scaling behavior in the critical regime. The parameters are the following: $\hbar = 2.89$, $\omega_2 = 2\pi\sqrt{5}$, $\omega_3 = 2\pi\sqrt{13}$, $K = 7.8$ and $\varepsilon = 0.3$. Color curves correspond to various choices of the phases φ_2 and φ_3 [see Eq. (1)] whereas the black curve results from a statistical average over different phases. The amplitudes of the quasi-resonant oscillations decrease as time goes on. Averaging over the phases kills the rapidly oscillating structures, while keeping all of the other dynamical properties unchanged.

most important correction to scaling is a time dependence of $\ln\Lambda$ at $K = K_c$ either due to (i) or (iii).

The well-known deviations (i) and (ii) can be taken into account by adding to (10) extra terms [17]. (i) The scaling function $\mathcal{F}$ depends not only on the relevant scaling variable χ_r (i.e. a function of $K - K_c$), but also on an irrelevant scaling variable ψ:

$$\ln\Lambda = \mathcal{F}\left(\chi_r t^{1/3\nu}, \psi t^{-y}\right) . \tag{11}$$

Since ψ is an irrelevant scaling parameter, its effects should vanish as t goes to infinity, thus y must be positive. (ii) Nonlinearity in the relevant scaling variable χ_r can be described by an expansion in terms $K - K_c$ up to order m_R.

To define a fitting function $\mathcal{F}_f$, we can then make a Taylor expansion of the scaling function $\mathcal{F}$ up to order n_R in $\chi_r t^{1/3\nu}$ and n_I in ψt^{-y}:

$$\mathcal{F}_f(K,t) = \sum_{m=0}^{n_R}\sum_{n=0}^{n_I} \chi_r^m t^{m/3\nu}\psi^n t^{-ny}\mathcal{F}_{m,n} . \tag{12}$$

We now discuss the qualitative nature of the correction due to the presence of an irrelevant scaling variable (i) as compared to the effect of resonances (iii). In case (i), $\ln\Lambda_c = \ln\Lambda(K = K_c)$ will shift in a monotonous way as time increases and converge to its thermodynamic limit $\ln\Lambda_c(t = \infty)$ [$\ln\Lambda_c(t) = \mathcal{F}_{0,0} + t^{-y}\mathcal{F}_{0,1}$ in the linear regime ($m_R = n_R = n_I = 1$)]. In the case of our three-frequency dynamical system, the data do not always fit such a monotonous evolution model for $\ln\Lambda_c(t)$. Indeed, for a generic choice of incommensurate periods, the data are found to oscillate around their transient anomalous diffusive dynamics, see Fig. 2.

We infer that such an oscillating correction to scaling arises in an resonant way: when the frequencies can be approximately related by a simple linear combination (i.e. involving small integers), a resonance occurs. This is a rather common phenomenon in multi-frequency dynamical systems. The phase and the amplitude of the oscillations in Fig. 2 depend on the choice of the phases φ_2 and φ_3 of the time-modulation [see Eq. (2)], i.e. on the initial state in Eq. (4). From the point of view of the Anderson-like model Eq. (7), resonances can be interpreted as correlations in the disordered potential. Hence, to perform the standard scaling analysis devised for the Anderson model with uncorrelated disorder [17], we shall retain data only for sufficiently long times and average over different initial conditions, i.e. different quasi-momenta and phases φ_2 and φ_3.

We computed $\ln\Lambda$ for times up to $t = 10^6$ kicks with an accuracy of 0.15%. To achieve this accuracy more than 1000 initial conditions are required. By discarding data for times $t \leq 1000$, an analysis of the data that neglects oscillating corrections becomes possible. To analyze data over the full range of times $t \in [10^3, 10^6]$, we fit the model Eq. (12) to the data. Note that the inclusion of the corrections (i) and (ii) in Eq. (12) leads to a rapid increase in the number of fitting parameters. That is why high quality data with a wide range of variation of $t^{1/3}$ are needed if meaningful fits are to be obtained.

The most likely fit is determined by minimizing the χ^2 statistics measuring the deviation, due to the numerical uncertainties, between the model and data. Some typical numerical data and the associated fit are displayed in Fig. 3. To exhibit scaling, we subtract the corrections due to the irrelevant scaling variable [17] obtaining the corrected quantity $\ln\Lambda_s$. As seen in Fig. 4, all data collapse almost perfectly on the scaling function deduced from the model $\mathcal{F}_f$.

No significant deviation of the scaling function from the fit is observed. The goodness of fit Q has been determined using the χ^2 distribution with $N_d - N_p$ degrees of freedom where N_d is the total number of data we used to fit the model [31] and N_p is the total number of fitting parameters (see Table 1). The confidence intervals for the fitted parameters were estimated using the bootstrap method which yields Monte-Carlo estimates of the errors in the fitted parameters [31]. In the following, we shall present the fitted parameters along with the corresponding 68.2% confidence intervals (one standard deviation).

Universality. – A key property of the Anderson transition is that it is a continuous (i.e. second order) phase-transition in which the critical behavior can be described in a framework of universality classes [5]. This means that the critical exponents should not be sensitive to the microscopic details of the disordered potential but should depend only on the underlying symmetries (e.g. time-reversal symmetry). We present here new material that allows us to numerically prove that this is indeed the case for the quasiperiodic kicked rotor, thus strengthening the fact that this system is in the same universality class than the truly random Anderson transition.

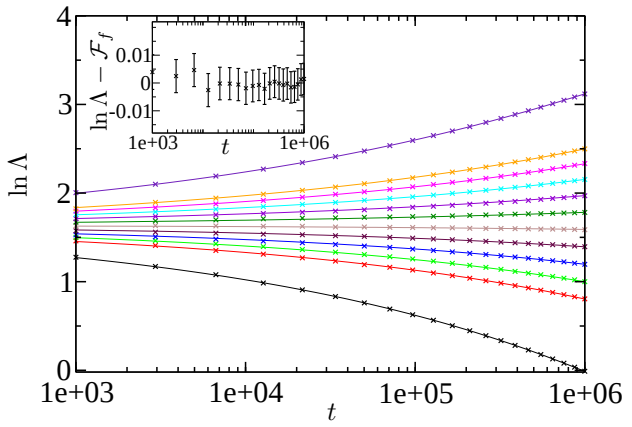

Fig. 3: (Color online) $\ln \Lambda$ as a function of time t. The **curves** are fits of the data according to the model $\mathcal{F}_f$ [see Eq. (12)] with $n_R = 3$, $m_R = 2$, $n_I = 1$. The parameters are that of the set $\mathcal{D}$ (see Table 1). The inset shows the deviations of the data (corresponding to $K = 7.9$) to the most likely fit, showing no statistically significant deviation.

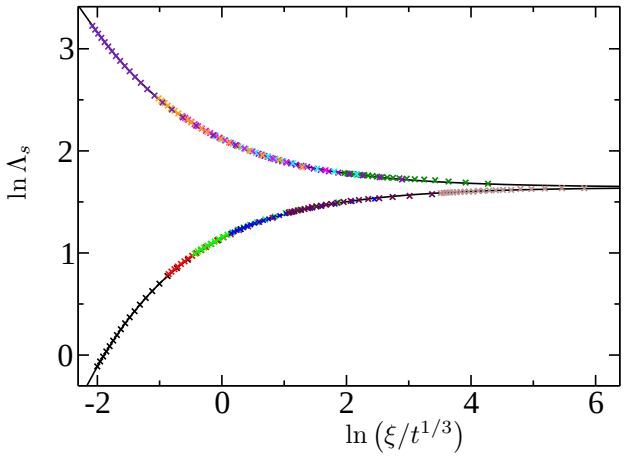

Fig. 4: (Color online) $\ln \Lambda_s$, the data in Fig. 3 after subtraction of corrections due to the irrelevant scaling variable, plotted versus $\ln\left(\xi/t^{1/3}\right)$ where $\xi = |\chi_r|^{-\nu}$ and the scaling function deduced from the model $\mathcal{F}_f$, Eq. (12) (black curve). The parameters are that of the set $\mathcal{D}$ (see Table 1). The best fit estimates of the critical stochasticity and the critical exponent are in this case: $K_c = 8.09 \pm 0.01$, $\ln \Lambda_c = 1.64 \pm 0.03$ and $\nu = 1.59 \pm 0.01$.

We have carried on a *detailed* study of four cases characterized by different set of parameters, see Table 1): $\mathcal{A}$ and $\mathcal{B}$ are both optimal set of parameters for experimental studies (see [16]), while $\mathcal{C}$ and $\mathcal{D}$ are rather for theoretical/numerical considerations. $\mathcal{C}$ is a first step towards an ideal choice of parameters: $\omega_2/\omega_3 = \eta$ where η is the silver number (see below), and the continuous fraction of $\hbar/\pi$ is constituted of small integers (to prevent the system to be close to a resonance). $\mathcal{D}$ should be a "best choice" of parameters if we seek the least correlations in the disorder Eq. (8). It is such that $\hbar$, ω_2, ω_3 and π are a "most incommensurate" *quadruplet* of numbers. As suggested in [14], we set $\hbar = \alpha$, $\omega_2 = \alpha/\eta$ and $\omega_3 = \alpha/\eta^2$ where $\eta = 1.324717...$ (the silver number which generalizes the golden number for triplet instead of pair of incommensurate numbers [32]) is the real root of the equation $\eta^3 - \eta - 1 = 0$, and $\alpha = 3.5399...$ is such that the continuous fractions of $\hbar/\pi = \alpha/\pi$, $\omega_2/\pi = \alpha/\eta\pi$ and $\omega_3/\pi = \alpha/\eta^2\pi$ are constituted of small (< 9) integers.

The details of the simulations and the types of fit used to analyze those sets are listed in Table 2. The estimated critical parameters and their confidence intervals are given in Table 3. Some *typical* data and scaling function are drawn in Figs. 3 and 4.

The most important point to be drawn from Table 3 is that the estimates of the exponent ν for the four different sets are in almost perfect agreement with each other and with the estimate of ν based on numerical studies of the truly random Anderson model $\nu = 1.57 \pm 0.02$ of the orthogonal symmetry class [17]. Note also that in the case of the quasiperiodic kicked rotor, the critical stochasticity K_c and $\ln \Lambda_c$ depend on: (i) the anisotropy governed by the parameter ϵ and (ii) $\hbar$, ω_2 and ω_3. The dependence (i) of the critical disorder and critical $\ln \Lambda$ on anisotropy is a typical feature of the Anderson transition in anisotropic solids [20]. The dependence (ii) follows from the relation between the initial "classical" diffusion constant and the parameters $\hbar$, ω_2 and ω_3 [24].

The Anderson transition with the quasiperiodic kicked rotor is a robust feature: indeed, the "naive" choices of parameters, set $\mathcal{A}$ and $\mathcal{B}$, lead to very clean critical behaviors, as clean as for the sophisticated choices of parameters, sets $\mathcal{C}$ and $\mathcal{D}$. Our experience is that for certain mutually incommensurate triplets ($\hbar$, ω_2, ω_3) systematic deviations to scaling (such as resonances) can occur for intermediate times, but eventually vanish.

Conclusion. – A numerical analysis of the critical behavior of the quasiperiodic kicked rotor has shown that this quantum chaotic system exhibits the same critical phenomena as the truly random Anderson model, i.e. both systems belong to the same (orthogonal) universality class [21]. By taking proper account of corrections to the scaling property around criticality, the universality of the critical exponent ν for the quasiperiodic kicked rotor was demonstrated. The critical exponent ν was determined with an accuracy better or comparable to the one achieved in previous numerical studies of the 3D-Anderson model [17, 19, 20]. Our result $\nu = 1.59 \pm 0.01$ is in perfect agreement with the value found for the orthogonal symmetry class [17]. It is clearly distinct from the value found for the unitary class $\nu = 1.43 \pm 0.04$ [19], and from the predictions $\nu = 1$ of the self-consistent theory of localization [34] and $\nu = 1.5$ of a recent ad-hoc refinement of the self-consistent theory [35].

	$\hbar$	ω_2	ω_3	K	ϵ
$\mathcal{A}$	2.85	$2\pi\sqrt{5}$	$2\pi\sqrt{13}$	$6.24 \to 6.58$	$0.413 \to 0.462$
$\mathcal{B}$	2.85	$2\pi\sqrt{7}$	$2\pi\sqrt{17}$	$5.49 \to 5.57$	$0.499 \to 0.514$
$\mathcal{C}$	2.2516	$1/\eta$	$1/\eta^2$	$4.98 \to 5.05$	$0.423 \to 0.436$
$\mathcal{D}$	3.5399	$\hbar/\eta$	$\hbar/\eta^2$	$7.9 \to 8.3$	$0.425 \to 0.485$

Table 1: The four sets of parameters considered: $\hbar$, ω_2 and ω_3 control the microscopic details of the disorder, while ϵ drives the anisotropy of the hopping amplitudes. In $\mathcal{C}$, $\omega_2/\omega_3 = \eta$ where η is the silver number (see below), and the continuous fraction of $\hbar/\pi$ is constituted of small integers. $\mathcal{D}$ is such that $\hbar = \alpha$, $\omega_2 = \alpha/\eta$ and $\omega_3 = \alpha/\eta^2$ where $\eta = 1.324717...$ is the silver number, i.e. the real root of the equation $\eta^3 - \eta - 1 = 0$, and α is such that the continuous fractions of $\hbar/\pi = \alpha/\pi$, $\omega_2/\pi = \alpha/\eta\pi$ and $\omega_3/\pi = \alpha/\eta^2\pi$ are constituted of small (< 9) integers [32].

	n_R	n_I	m_R	N_d	N_p	χ^2_r	Q
$\mathcal{A}$	3	1	2	800	12	236	1
$\mathcal{B}$	2	1	1	600	9	278	1
$\mathcal{C}$	2	1	1	1000	9	934	0.9
$\mathcal{D}$	3	1	2	1212	12	917	0.999

Table 2: Parameters used for the four sets of data: type of fit [see Eq. (12)], number of data points N_d, number of parameters N_p, value of χ^2_r for the best fit and goodness of fit Q. Time ranges from $t = 10^3$ to $t = 10^6$.

	K_c	$\ln \Lambda_c$	ν	y
$\mathcal{A}$	6.36 ± 0.02	1.60 ± 0.04	$\mathbf{1.58 \pm 0.01}$	0.71 ± 0.28
$\mathcal{B}$	5.53 ± 0.03	1.08 ± 0.09	$\mathbf{1.60 \pm 0.03}$	0.33 ± 0.30
$\mathcal{C}$	5.00 ± 0.03	1.19 ± 0.15	$\mathbf{1.60 \pm 0.02}$	0.23 ± 0.29
$\mathcal{D}$	8.09 ± 0.01	1.64 ± 0.03	$\mathbf{1.59 \pm 0.01}$	0.43 ± 0.23

Table 3: Best fit estimates of the critical parameters K_c and $\ln \Lambda_c$, the critical exponent ν together with their uncertainty (one standard deviation). ν is expected to be universal whereas $\ln \Lambda_c$ and K_c do depend on anisotropy [33] and $\hbar$, ω_2 and ω_3. Irrelevant parameters are sensitive to microscopic details, therefore y is strictly positive and not universal.

* * *

We thank J.C. Garreau, P. Szriftgiser, J. Chabé, H. Lignier and F. Farago for many interesting and fruitful discussions.

REFERENCES

[1] Anderson P. W., *Phys. Rev.* , **109** (1958) 1492.

[2] Fishman S., Grempel D. R. and Prange R. E., *Phys. Rev. Lett.* , **49** (1982) 509.

[3] Casati G., Guarneri I., Izrailev F. and Scharf R., *Phys. Rev. Lett.* , **64** (1990) 5.

[4] Fyodorov Y. V. and Mirlin A. D., *Phys. Rev. Lett.* , **67** (1991) 2405.

[5] Efetov K., *Supersymmetry in Disorder and Chaos* (Cambridge University Press, Cambridge, UK) 1997.

[6] Altland A. and Zirnbauer M. R., *Phys. Rev. Lett.* , **77** (1996) 4536.

[7] Janssen M., *Physics Reports* , **295** (1998) 1 .

[8] Hefei H., Strybulevych A., Page J. H., Skipetrov S. E. and van Tiggelen B. A., *Nature Phys.* , **4** (2008) 945.

[9] Chabanov A. A., Stoytchev M. and Genack A. Z., *Nature (London)* , **404** (2000) 850.

[10] Wiersma D. S., Bartolini P., Lagendijk A. and Righini R., *Nature (London)* , **390** (1997) 671.

[11] Störzer M., Gross P., Aegerter C. M. and Maret G., *Phys. Rev. Lett.* , **96** (2006) 063904.

[12] Schwartz T., Bartal G., Fishman S. and Segev B., *Nature (London)* , **446** (2007) 52.

[13] Moore F. L., Robinson J. C., Bharucha C., Williams P. E. and Raizen M. G., *Phys. Rev. Lett.* , **73** (1994) 2974.

[14] Wang J. and García-García A. M., *Phys. Rev. E* , **79** (2009) 036206.

[15] Casati G., Guarneri I. and Shepelyansky D. L., *Phys. Rev. Lett.* , **62** (1989) 345.

[16] Chabé J., Lemarié G., Grémaud B., Delande D., Szriftgiser P. and Garreau J. C., *Phys. Rev. Lett.* , **101** (2008) 255702.

[17] Slevin K. and Ohtsuki T., *Phys. Rev. Lett.* , **82** (1999) 382.

[18] Basko D. M., Skvortsov M. A. and Kravtsov V. E., *Phys. Rev. Lett.* , **90** (2003) 096801.

[19] Slevin K. and Ohtsuki T., *Phys. Rev. Lett.* , **78** (1997) 4083.

[20] Milde F., Römer R., Schreiber M. and V. U., *Eur. Phys. J. B* , **15** (2000) 685.

[21] Evers F. and Mirlin A. D., *Rev. Mod. Phys.* , **80** (2008) 1355.

[22] Scharf R., *J. Phys. A* , **22** (1989) 4223.

[23] Blümel R. and Smilansky U., *Phys. Rev. Lett.* , **69** (1992) 217.

[24] Shepelyansky D. L., *Phys. Rev. Lett.* , **56** (1986) 677.

[25] Abrahams E., Anderson P. W., Licciardello D. C. and Ramakrishnan T. V., *Phys. Rev. Lett.* , **42** (1979) 673.

[26] MacKinnon A. and Kramer B., *Phys. Rev. Lett.* , **47** (1981) 1546.

[27] Pichard J. L. and Sarma G., *J. Phys. C* , **14** (1981) L127.

[28] Stauffer D. and Aharony A., *Introduction to Percolation Theory* 2nd Edition (Taylor and Francis) 1994.

[29] Wegner F., *Z. Phys. B*, **25** (1976) 327.

[30] Ohtsuki T. and Kawarabayashi T., *J. Phys. Soc. Jpn.* , **66** (1997) 314.

[31] Press W. H., Teukolsky S. A., Vetterling W. T. and Flannery B. P., *Numerical Recipes in Fortran. The art of scientific computing* 2nd Edition (Cambridge University Press, Cambridge, UK) 1992.

[32] Kim S.-h. and Ostlund S., *Phys. Rev. A* , **34** (1986) 3426.

[33] Panagiotides N. A., Evangelou S. N. and Theodorou G., *Phys. Rev. B* , **49** (1994) 14122.

[34] Vollhardt D. and Wölfle P., *Phys. Rev. Lett.* , **48** (1982) 699.

[35] García-García A. M., *Phys. Rev. Lett.* , **100** (2008) 076404.